RESEARCH ARTICLE

Open Access

Correlation between air temperature and surface ozone in their extreme ranges in the greater Tokyo region

Hiroshi Yoshikado[1]*

Abstract

High-level ozone (O_3) events observed around major urban regions in the middle latitudes are correlated with high temperatures (T-O_3 correlation). Therefore, the effects of global warming on the future O_3 levels are a matter of concern. The T-O_3 correlation is caused by various physicochemical and meteorological processes, the importance of which can differ by region. This statistical analysis focused on the correlation in the extremely high ranges, because the lower ranges would only act as noise in elucidating the conditions at which high temperatures and high levels of O_3 occur. This methodology was applied to the greater Tokyo region after 2001, where severe O_3 events frequently occurred when the sea breeze system developed in summer. To select sample days for the analysis, this study set up twofold filtering: (1) a large threshold for midday sunshine duration and (2) a typical variation pattern to roughly judge sea breeze days, mostly essential weather pattern for high-level O_3 events in the region. The most notable result was a decrease in O_3 corresponding to the reduction in non-methane hydrocarbons (NMHC) from Period I (2001–2007) to Period III (2017–2019). As the NMHC rank reduced, the linear regression line for the T-O_3 correlation shifted downward, but its slope (ppb/°C) remained around 10, except that temporary spikes in O_3 levels and temperatures occurred at moderate NMHC levels. From an urban meteorological perspective, the wind speed in the mature stage of the sea breeze is the major factor behind the T-O_3 correlation.

Highlights

• Daily maximum temperature-ozone correlation in a large urban region after 2001.

• Temperature-O_3 correlation focused on typical meteorological pattern in summer.

• Reduction of O_3 precursors not influences the slope of temperature-O_3 correlation.

• Sea breeze advance velocity is a major factor causing temperature-O_3 correlation.

Keywords Ozone, Precursor reduction, Temperature-ozone correlation, Greater Tokyo region, Sea breeze

1 Introduction

Around the major urban regions located in the middle latitudes, high levels of ozone (O_3) frequently occur during the daytime in summer. Increases in ambient O_3 are caused by complex photochemical reactions of the precursors, mainly volatile organic compounds (VOCs) and nitrogen oxides (NO_x), emitted in the region. The reactions depend on solar radiation intensity. Simultaneously, the solar radiation affects various processes near

*Correspondence:
Hiroshi Yoshikado
tceat.yos@gmail.com
[1] National Institute of Advanced Industrial Science and Technology, Tsukuba, Ibaraki 305-8569, Japan

the ground surface, particularly the increase in air temperature. Therefore, a positive correlation between air temperature and O_3 concentration (T-O_3 correlation) is generally observed. The T-O_3 correlation has led to concerns about the influence of higher temperatures on summer O_3 levels, which is associated with global warming. This problem was termed as the "O_3 climate penalty" and has been actively discussed (e.g., Kerr et al., 2019; Porter & Heald, 2019; Rasmussen et al., 2012). The main subject of these studies is the relative importance of various processes responsible for the T-O_3 correlation, because it does not represent a direct connection between them but is a synthetic result of many processes affected by solar radiation and temperature. For example, VOC emissions from many sources increase with temperature rise, which promotes O_3 production. Relative importance of the relevant processes can be different in every region, and no universal ranking is supposed to be significant. Therefore, area-specific research can provide valuable insights.

This study focused on the T-O_3 correlation observed in the greater Tokyo region and explored the changes in the correlation and their causes by using monitoring data after 2001. Dense and well-maintained monitoring data were obtained there. Notably, its T-O_3 correlation has not been investigated except a few brief reports (Yonemochi, 2019); thus, this study affords contribution to the literature. Before conducting the T-O_3 correlation analysis for a specific region, we fixed the methodology for the analysis. A discussion of the methodology is presented in Sect. 2. A brief introduction to tropospheric O_3 in the greater Tokyo region is as follows.

Tokyo and its downwind areas have long experienced severe air pollution. Since the 1970s, photochemical air pollution warnings have been issued most frequently in the country, and this region was the main target of countermeasures for reducing photochemical O_3. Accordingly, high-level O_3 events in the region were studied repeatedly (e.g., Inoue et al., 2010; Kiriyama et al., 2015; Ueno & Tsunematsu, 2019; Wakamatsu et al., 1999). The basic structure and behavior of those events are localized within the Kanto Plain, although long-range transport from the Asian continent is occasionally observed in spring (Itahashi et al., 2009). The major sources of O_3 precursors are distributed in the southern part of the plain including the Tokyo metropolitan area. In contrast, the areas where O_3 reaches maxima extend from the source area to the northern part of the plain. This northward expansion of the pollution is almost solely brought by the southerly sea breeze prevailing during the daytime in the warm seasons (e.g., Kurita & Ueda, 1986; Wakamatsu et al., 1981). The sea breeze in this region is occasionally organized in a terrain-induced thermal low covering Central Japan (Kondo, 1990). Furthermore, light gradient winds from the Western Pacific high support the sea breeze to extend, although its effect is changeable.

2 Selection of sample days for the analysis

2.1 Daily-base sampling
The selection of samples for analysis is a fundamental factor in this methodology. Daily sets of reference values for various properties are mostly basic samples. Long-term data are often organized as monthly or annual averages. However, averaged datasets do not necessarily provide suitable features. For example, Ooka et al. (2011) demonstrated a strong correlation between the average daily maximum temperature (T_{max}) and maximum O_3 concentration for the summer months of every year between 1985 and 2005. However, these averaged values can be mutually correlated through their dependences on the number of clear-sky days (cloud cover less than a fixed value), even if high temperatures and O_3 levels do not occur. Specifically, the correlation obtained from yearly averaged data does not purely reflect physicochemical processes (Yoshikado, 2021). Changes in future O_3 level that can occur with warming should be examined as a result of physicochemical processes on a daily basis rather than long-term average properties. Therefore, the analysis used samples from a daily dataset.

2.2 Selecting clear-sky days
The most important factor of temperature and O_3 production is solar energy. It can be measured by sunshine duration (SS) or, more precisely, solar radiation intensity. The T-O_3 correlation is a composite of T- and O_3-dependences on SS. Accordingly, any variation in T and O_3, irrespective of the abundance of SS, can disturb the T-O_3 correlation. In addition to meteorological conditions, seasonal transitions such as changes from early summer to mid-summer, spatiotemporal variations in precursors, and other factors can cause such disturbances. In other words, even during hot seasons when severe O_3 events frequently occur, the relationship between temperature and O_3 level under cloudy-sky conditions should be considered to have a different system from that on clear-sky days. Because the response of the O_3 level to climatic warming is of interest, focusing on the T-O_3 correlation in the high-temperature range is a reasonable choice. Restriction of statistics to "clear-sky days" is also a suitable choice. Consequently, most of our analyses applied a threshold to the SS of the sample days. Detailed data information is given in Sect. 3.

2.3 Selecting sea breeze days
Diversity of wind systems prevalent in the region can be a major factor disturbing the T-O_3 correlation. In other words, different wind systems contribute to each specific

T-O_3 correlation. In coastal source areas, onshore gradient winds generally tend to lower the temperature and raise the inland-side O_3 concentrations, whereas offshore gradient winds raise temperature and lower O_3. Specifically, in the greater Tokyo region, onshore sea breezes prevail on summer days (e.g., Kurita & Ueda, 1986; Yoshikado, 2013), and high-level O_3 events typically occur under those conditions (Khiem et al., 2010). Therefore, as a final step, days on which the sea breeze system satisfied a fixed definition, and the lowest limit of *SS* was exceeded as mentioned in the foregoing subsection, were selected as samples for our analysis. Details of the applied conditions are described in Sect. 3.3.

3 Geography of the region and used data

3.1 Region and monitoring sites

The metropolitan area of Tokyo is located along the northwest corner of Tokyo Bay, and greater Tokyo extends northwest and along the bay shore (Fig. 1). Photochemical O_3 is generally produced in the sea breezes developing from Tokyo and Sagami bays. These sea breezes vary in intensity and extent under the influence of a synoptic-scale pressure gradient that decreases northward and the heat-island effect of the metropolitan area (Yoshikado, 1992). Thus, O_3 maxima are observed mostly within the urban areas or northern suburbs. The eastern parts of the Tokyo and Saitama prefectures (cf.

Figure 1) correspond to the highest O_3 zone, which can be arbitrarily divided into S, M, and N sub-areas. For determining the maximum level in the region, 18 representative O_3 monitoring sites were selected. The maximum "level" was obtained as the average of the first and the second largest (hereinafter referred to as Top 2) daily maximum 1-h O_3 records from the 18 sites because a peak value from a single monitoring site might simply represent localized irregularities.

The main sources of O_3 precursors are distributed in and around the metropolitan area (sub-area S), where 13 monitoring sites measuring hourly non-methane hydrocarbons (NMHC, used as a substitute for VOCs) and NO_x are in operation. The average NMHC and NO_x of 13 sites were used in this study.

The daily maximum hourly record of *T* from the Saitama-Urawa automated station (AMeDAS) was employed as a representative. Hourly *SS* and wind (speed and direction) data were sourced from the Saitama-Urawa and Tokyo AMeDAS. *SS* was used to select clear-sky days and in the process selecting sea breeze days. Detailed judgment flows are presented in Sect. 3.3.

3.2 Data periods analyzed

Since our prime concern was the increase in O_3 on hot summer days, all 62 days in July and August of every summer were selected as the first stage. June was excluded
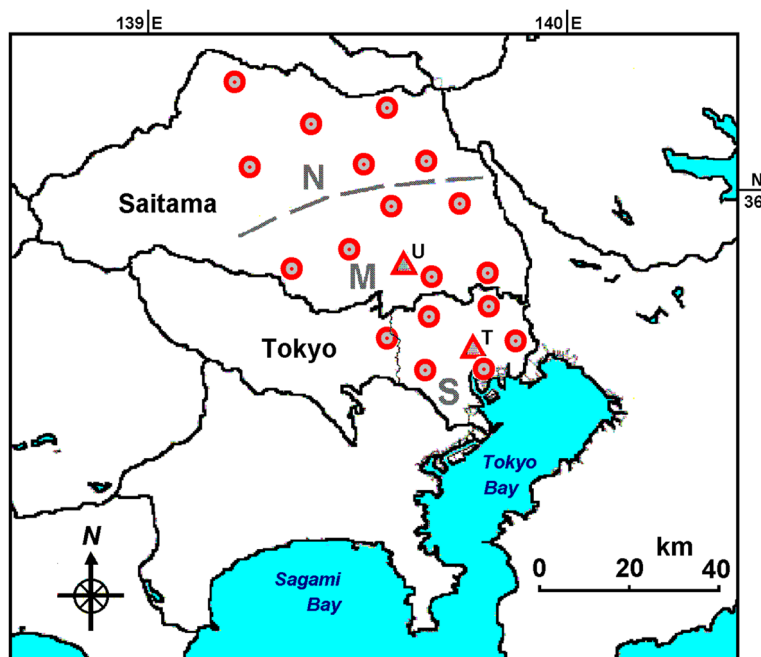

Fig. 1 Monitoring sites used in the study as representatives of O_3 in South (S, eastern Tokyo), Middle (M, south-eastern Saitama), and North (N, North-eastern Saitama) sub-areas, and the automated meteorological sites (AMeDAS) in Tokyo (T) and Saitama-Urawa (U). Thirteen monitoring sites, from which average levels of NMHC and NO_x were obtained, were all in the S sub-area

because it is a rainy month in Central Japan. April and May were also used for reference because the weather in the region is generally fair and high-level O_3 events occasionally occur even without very high temperatures in these spring months. March has a considerably different climate, and hence, it was excluded here. Relevant data from 2001 to 2019 were available to examine recent trends.

The 3-h averages of the O_3 precursors during 0600–0900 JST (hereafter referred to as 06–09 h) were used as reference values to measure the effect on O_3 production until midafternoon. The recent trends are shown in Fig. 2. Both the NMHC and NO_x decreased overall, specifically, in a stepwise manner, with relatively flat curves during Periods I and II.

Variations in precursors influence the relationship between T and O_3. The ratio NO_x/NMHC (Fig. 3) increased between Periods I and II as a result of the effective reduction in NMHC compared to that in NO_x. According to Inoue et al. (2019), the O_3 formation regime in the Tokyo metropolitan area was VOC sensitive during the early stages of this century. Therefore, the conspicuous reduction in NMHC (in place of VOC in this study)

might have been a significant countermeasure to high levels of O_3, as confirmed in Sect. 4.3. Wakamatsu et al. (2013) provided a historical review of these measures.

However, based on the regression lines in Fig. 3, the ratio NO_x/NMHC changed only within a range of 0.13 to 0.17, which can be said no substantial variation. For reference, Sakamoto et al. (2019) reported the ratio at which the O_3 production regime switches to be approximately 0.067 (the inverse ratio 15). Therefore, the ratio range in this study was sufficiently far from the regime transitional zone, and only the NMHC data are referred to in the following section of the analysis. Periods I and II were selected for the correlation analysis. Additionally, Period III was examined to determine the most recent situation, although this period was shorter than the others.

3.3 Clear-sky days and sea breeze days
In accordance with the methodology stated in Sect. 2, the "clear-sky days" were selected from the whole summer days (partially with spring days) in the three periods for further analysis. A "clear sky" was defined as follows: SS (expressed by the rate of 0–10 for every hour) reached or
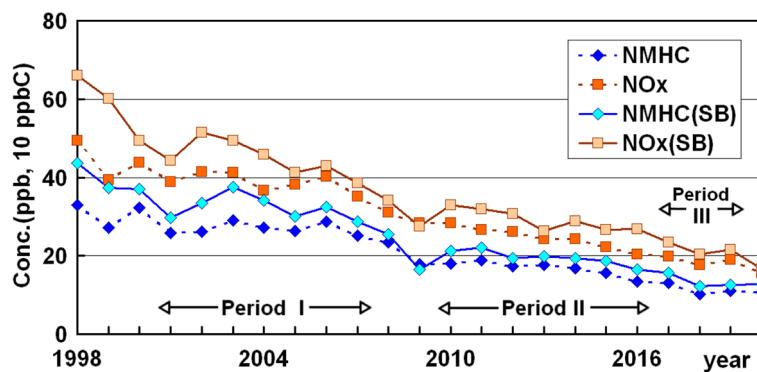

Fig. 2 Trends in the reference values of the O_3 precursors in summer (averages of all the available 13 monitoring sites for NMHC, where NO_x is also measured). Cases denoted by "SB" indicate averages for exclusive sea breeze days and the others for the whole 62 days
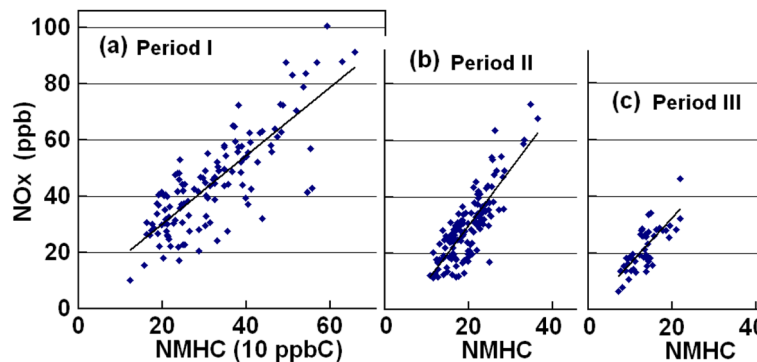

Fig. 3 Daily reference values for NMHC vs. those for NO_x for the summer SB days for Period I–III

exceeded 45 (max. 60) when summed over 6 h between 09 and 15 h (*SS*6h) at both the Tokyo and Urawa sites.

All days in the periods were classified into two groups: sea breeze (SB) days and non-SB days, to characterize atmospheric transport in the region. Only the SB days with SS6h $\geq$ 45 were considered for the *T*-O$_3$ correlation analysis. Here, a composite of several conditions was applied to identify SB days. It was originally established by Yoshikado (2013) and is described as follows:

i)   *SS*6h $\geq$ 30, not as large as the threshold for clear-sky days
ii) The wind at the Tokyo site was northerly (WSW–E clockwise), or less than 4.5 ms^{-1} during 04–06 h, and item (iii) did not start before 08 h.
iii) The wind changed to southerly (ESE–SW clockwise) between 08 and 14 h and persisted for two consecutive hours or longer at a speed faster than 2 ms^{-1}.
iv) At the Urawa site, conditions similar to (i)–(iii) for the Tokyo site were satisfied, but the onset of the southerly wind in (iii) was not earlier than that at the Tokyo site.

Conditions (i)–(iv) reflect the empirically established fact that the sea breeze system tends to develop under clear skies with light gradient wind, but not with predominant gradient winds, even under clear skies.

3.4 Reference values characterizing sample days
There could have been arbitrariness in finding reference values that represented each sample day in the analysis. Meteorological factors *T* and *SS* were generally slightly localized in representing daily conditions in the region, and two AMeDAS stations were selected as indicated above. The daily maximum *T* (T_{max}, precisely, largest hourly *T*) near the regional center (U in Fig. 1) was employed for the *T*-O$_3$ correlation analysis. Although an average *T* during the daytime might be more appropriate to connect with daily O$_3$ production, T_{max} and average *T* were correlated with a correlation coefficient *R* > 0.95. Data representing the air pollutants are presented in Sect. 3.1. Additional comments regarding the maximum level of O$_3$ are provided below.

The area where high-level O$_3$ events occur is generally changeable, even within a day and from day to day, in the region shown in Fig. 1. As a reference value of O$_3$, "Top 2" from the whole region was employed (Sect. 3.1). A preliminary examination compared the Top 2 and the maximum daily 8-h average O$_3$ (MDA8), a frequently used reference, resulting in a high correlation (*R* larger than 0.95) for the entire region. In the comparison at each station, *R* tended to be smaller.

4 Results
4.1 Sample groups during three periods
In the first stage, four sample sets consisting of clear-sky SB days were obtained from Periods I (2001–2007) and II (2010–2016), as shown in Table 1. Although SB days occurred roughly every 3 days in both spring and summer, clear-sky condition (SS6h $\geq$ 45/60) reduced the final number of samples, especially in summer. Specifically, even in SB cases, cloudy skies partially extended more frequently in summer. The sample size was not sufficiently large for statistical analysis. To supplement the summer samples, especially considering the more recent circumstances in the study, the fifth sample set from Period III (2017–2019) was added later, although this period was shorter than that of the others.

Table 1 Number of days included in each category

Season	Spring		Summer		
	(April-May)		(July-August)		
Period[*1]	I	II	I	II	III
Sample total	427	427	434	434	186
Data incomplete	2	3	0	1	1
Sea breeze days	134	146	126	141	49
SS6h[*2] $\geqq$ 45	166	180	118	145	52
Sea breeze days[*3]	101	105	65	84	27

[*1]) Period I: 2001-2007, II: 2010-2016, III: 2017-2019

[*2]) Total of 1 h sunshine rate during 09-15 h (max.: 60) both at Tokyo and Saitama

[*3]) Number with SS6h $\geqq$ 45

4.2 Overview of Periods I and II

The T-O_3 correlations for Periods I and II are shown in Fig. 4. Overall, the daily maximum levels in O_3 (Top 2) increased with the daily maxima in T and were lower in Period II than in Period I. Dispersions were fairly small as a result of twofold screening by SS and the wind system (SB). The spring and summer samples lay together in series, although their T ranges were mostly different. While the O_3 plots lay smoothly along the linear regression lines in spring (slope 4.53 and 3.31 ppb/°C), those in summer had steeper lines. The variances in summer appeared to be very large owing to their narrow T ranges. When the summer plots in Fig. 4 were observed on a wider horizontal axis, there was a phase shift at approximately 33 °C; the samples exceeding 33 °C had much steeper regression lines than those in spring, whereas those below 33 °C acted similarly to the spring samples.

Therefore, the high T range (≥ 33 °C) should be further examined.

4.3 *Response to the reduction in O_3 precursors*

The large variances in the T-O_3 correlations for the summer cases resulted from the narrow T range between 33 and 38 °C, and wide variation in O_3, even within the set of clear-sky SB days. The primary factor dominating O_3 production was the precursor level at the initial stage of O_3 production. This is largely influenced by local meteorology (Yoshikado, 2015).

The T-O_3 correlation of the part $T \geq 33$ °C is shown again in Fig. 5 after regrouping by four ranks (cf. Table 2) of the NMHC reference value (Sect. 3.2). All sample days of rank 4 occurred in Period I, and most of the rank 2 samples occurred in Period II. Rank 3 occurred during Periods I and II, representing a transition between these
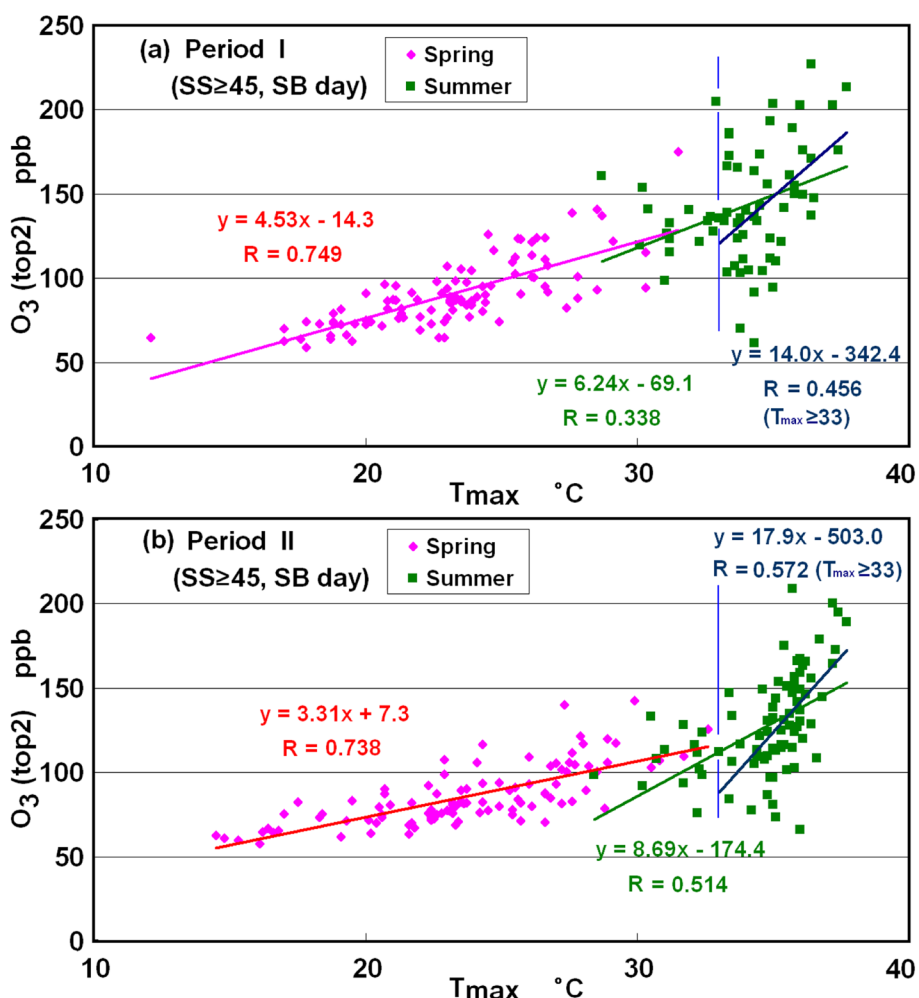

Fig. 4 **a** T_{max} vs. daily maximum O_3 (Top 2) for Period I. The clear-sky SB days in spring and summer are plotted with different colors. Linear regression lines for spring, summer, and cases $T_{max} \geq 33$ °C in summer are shown along with the respective statistics. **b** Same as in (a) except for Period II
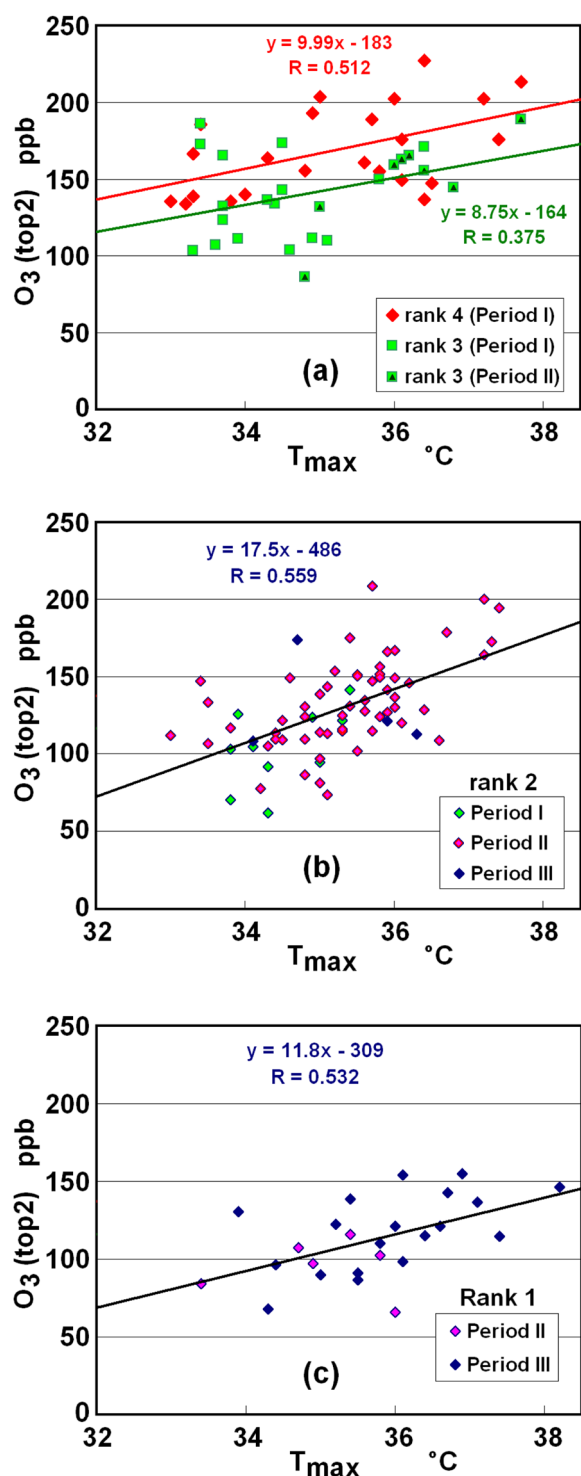
Fig. 5 T_{max} vs. daily maximum O_3 (Top 2) for the section $T_{max} \geq 33$ °C after grouping by four ranks of the NMHC reference value. **a** NMHC rank 4 (0.35–0.65 ppmC), occurred only in Period I, and rank 3 (0.25–0.35 ppmC) in Periods I and II. Regression lines correspond to the rank of the same color symbol. **b** NMHC rank 2 (0.15–0.25 ppmC). **c** NMHC rank 1 (0.05–0.15 ppmC)

two periods. As indicated by the relative positions of the regression lines, the O_3 level decreased with an increasing NMHC rank. However, the slope for rank 2 (Fig. 5b), 17.5 ppb/°C, was abnormally larger than the others. This change can be traced to several events of high O_3 exceeding 150 ppb in the highest T range that occurred in Period II. Specifically, the O_3 level in this T range did not decrease conspicuously along with the decrease in the NMHC. This may have been associated with climatic fluctuations over a short period. Further discussion is provided later in connection with Fig. 6a.

In Period II, a few sample days fell into rank 1. Therefore, those in Period III were supplemented with the most recent summers, as shown in Fig. 5c. The regression line for these data tended to be parallel (slope approximately 10 ppb/°C) to those of ranks 3 and 4 but not to that of rank 2, although only few sample days distributed in the highest T range.

Even after sub-grouping the samples by NMHC rank, the variances in O_3 were somewhat large, and the correlation coefficients (R) were not sufficiently large: from ranks 4 to 1, $R = 0.51$, 0.37, 0.56, and 0.53. According to a detailed analysis of sample days that largely deviated from the regression line (Yoshikado, 2021), their wind patterns were quite irregular, even though they satisfied the sea breeze criteria described in Sect. 3.3. The main point of irregularity was the large delay of sea breezes in reaching the inland site of Urawa.

The O_3 values at 35 °C, the approximate middle point on the regression lines in Fig. 5, were, from the highest NMHC rank, 167, 142, 125, and 104 ppb. Specifically, reductions in the NMHC rank of every 0.1 ppmC interval with roughly parallel reductions in NO_x caused a reduction in O_3 of approximately 20 ppb.

4.4 One major factor responsible for the T-O_3 correlation

As mentioned above, the variance in O_3 in Fig. 5 appears to be magnified by cases of late inland penetration of sea breezes. Considering that slow penetration mostly corresponds to a small SB velocity in the coastal area, the wind speed at the Tokyo site averaged for four hourly records of 13–16 h (W_{ave} 13–16) was selected as representative.

Figure 6 shows a re-examination of Fig. 5 for NMHC ranks 1 and 2 separated by the SB velocity at 4.5 ms^{-1}. At lower wind speeds (Fig. 6a), the regression line was lifted by very high levels of O_3, although the variance was large. When Fig. 5b is compared with Figs. 6a and b, most sample days above 160 ppb of O_3 are found in the lower velocity case (Fig. 6a). Furthermore, deeper inspections revealed that these sample days tended to occur in succession within several days as well as during specific summers. This suggests that the large slope for NMHC rank 2 (Fig. 5b) could be associated with climatic fluctuations

Table 2 Number of sample days[*1] (SS6h ≥ 45, SB days) classified to four ranks of the NMHC reference value[*2] with the correlation coefficient (*R*) and the slope of regression (*S*)

NMHC rank	range[*3] (ppmC)	Period[*4]			total (days)	*R* (−)	*S* (ppb/°C)
		I	II	III			
4	0.35- 0.65	23	0	0	23	0.512	10.0
3	0.25- 0.35	17	8	0	25	0.375	8.75
2	0.15- 0.25	10	57	4	71	0.559	17.5
1	0.05- 0.15	0	6	19	25	0.532	11.8
	(total)	50	71	23	144		

[*1]) Excluding the cases T_{max} less than 33 °C

[*2]) 3-h average concentration during 06-09 h

[*3]) The upper limits are not included (i.e., less than)

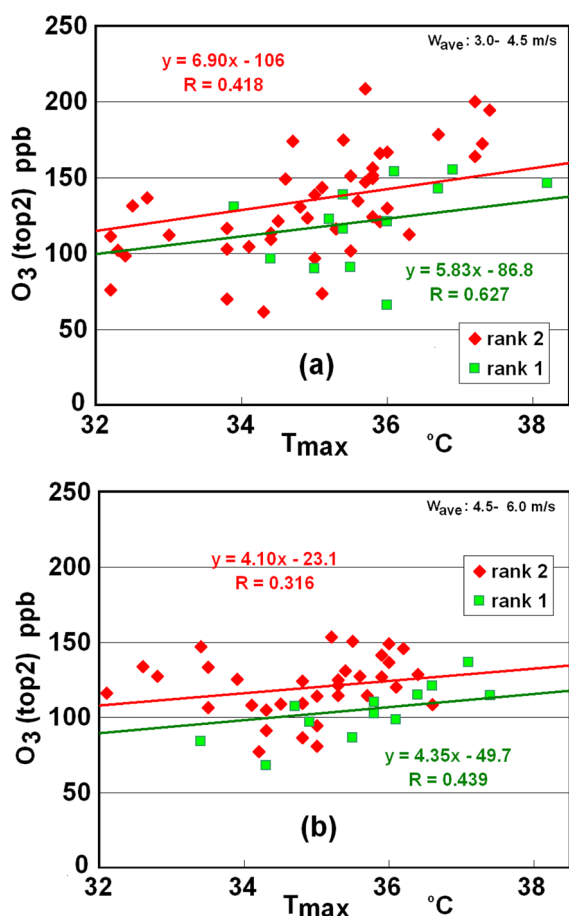[*4]) Period I: 2001-2007, II: 2010-2016, III: 2017-2019

Fig. 6 Rearrangement of Fig. 5b and c with respect to the SB velocity. **a** W_{ave}13–16 ranged within 3–4.5 ms^{-1} and **b** ranged within 4.5–6 ms^{-1}. Here, the regression analysis data are from the whole T_{max} range

characterized by low SB velocities. Further analysis is required to determine the effects of short-period climate (typically associated with ENSO) on O_3 trends.

Figure 7 shows how sea breeze intensity affects the extreme increases in *T* and O_3. The symbols indicate sub-areas S, M, and N (cf. Figure 1) where O_3 exceeded 120 ppb for two successive hours at two or more of the six sites. The general tendencies are as follows.

i) The occurrence rate of high-level O3 events above 120 ppb (colored symbols) is high at lower wind velocities; in contrast, that of low-level O3 (symbol x) is high at higher wind velocities.

ii) High temperatures in the extreme range occur at low wind velocities and are accompanied by high-level O_3 events in most cases.

iii) High-level O_3 events at low wind velocities mostly occur in the S sub-area where the urban center is located (in addition to S, symbols SM and SMN indicate its occurrence in the S sub-area). Even under intense sea breezes, O_3 occasionally reached high levels in the N sub-area.

The factors enhancing summer heat around a large urban region presumably aid in understanding the T-O_3 correlation in the highest temperature range. Yoshikado (1992) provided a perspective from urban meteorology regarding the behavior of the sea breeze in the greater Tokyo region. Generally, the southerly gradient wind cooperates with the sea breeze to pass through the urban center by noon or early afternoon. However, under a light gradient condition, the urban heat island along the coast prevents the sea breeze from passing through, during which a stagnant area forms over the northern suburbs. This stagnant condition intensifies warming and simultaneously causes the accumulation of air pollutants in the urban and northern suburban regions. Findings (i)–(iii)
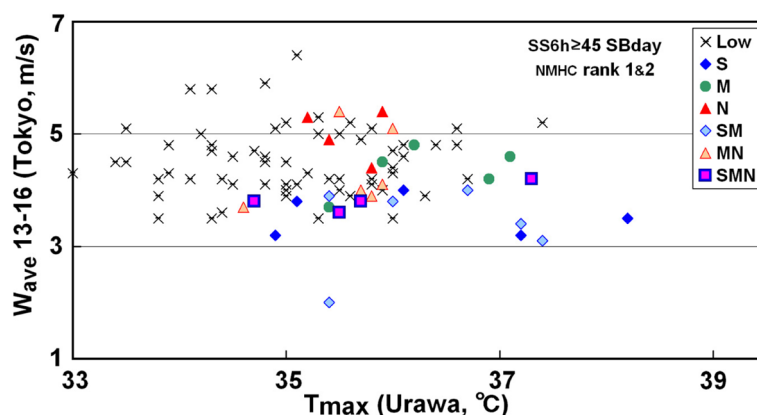
Fig. 7 T_{max} vs. W_{ave}13–16 on the clear-sky SB days (NMHC ranks 1 and 2). Symbols indicate the sub-area(s) where high-level O_3 events occurred

based on Fig. 7 support the idea that a smaller SB velocity, or the formation of a stagnant area by the urban effect, intensifies both urban temperature and high-level O_3.

Although the contribution of stagnation to the T-O_3 correlation has been discussed as an important factor (e.g., Coates et al., 2016; Garrido-Perez et al., 2019; Pusede et al., 2015), no specific meteorological structure has been described. The present case establishes the behavior of the sea breeze as a major factor responsible for the T-O_3 correlation over a single heavily urbanized region.

5 Discussion and conclusion

The T-O_3 correlation has been broadly recognized. Therefore, the effects of global warming on future O_3 levels are concerning. In further research, investigations of the mechanisms responsible for intense heat in selected regions, and temperature-dependent factors raising O_3 levels, are required. As a distinctive methodology, the present study focused on the T-O_3 correlation for summer days within specific ranges of T_{max} and SS and furthermore with specific wind patterns.

In the greater Tokyo region, the daytime peak of O_3 decreased as the emissions of the O_3 precursors decreased, except for temporary persistence recorded under very hot conditions in Period II (2010–2016). A tentative interpretation of this exception was given in Sect. 4.4. In the most recent period, Period III (2017–2019), the precursors were further reduced to the NMHC rank 0.05–0.15 ppmC in most cases, and no irregularly high O_3 was found in the very high-temperature range. Therefore, the T-O_3 correlation can be summarized generally as the slope of the regression line of approximately 10 ppb/°C over a considerably wide range of variations in the precursors since 2001. These large slope values resulted from the daily maximum in O_3 and the daily maximum temperature on clear-sky days, ranging within 33–38 °C, and were not comparable with those based on the maximum daily 8-h average O_3 (MDA8) and nonspecific weather conditions (e.g., Bloomer et al., 2009; Ninneman & Jaffe, 2021). Because the ratio of MDA8 to daily maximum was approximately 0.7 from the preliminary analysis, the slope on the MDA8 base could be approximately 7 ppb/°C, still larger than those in literature, such as 0–6 (Kerr et al., 2019). If T_{max} on clear-sky summer days rises owing to global warming, the large slope of the regression of the T-O_3 correlation in the high-temperature range examined in this study will be of significance. However, Otero et al. (2021) reported that the slope decreases with the reduction in O_3 precursors. Furthermore, the inverse view that the O_3 level does not rise much more in a higher temperature range (e.g., Steiner et al., 2010) needs examination. The realities of these findings depend on future data accumulated in various regions.

In addition to the precursors level dominating O_3 production, this study focused on the contribution of local meteorology to O_3 increase, major factor of which was the sea breeze intensity. The southerly gradient wind superposed on the sea breeze; therefore, the behaviors of the Western Pacific high as its source, are dominant factors. Fine weather in summer (typically, SS6h $\geq$ 45) is also accompanied by this high-pressure system. Therefore, if the summertime predominant pressure distribution changes, its prediction will be a key point when considering its dominant influence on the sea breeze behaviors.

The present data suggest that the frequency of high levels of O_3 will be low as long as the decreasing trend in the precursors is maintained. However, we cannot predict about the situation where "very hot days" frequently occur due to global warming because such sample days hotter than 38 °C are still rare.

Another limitation of the present analysis is that the precursors were represented by NMHC data. Ueno and Tsunematsu (2019) reported that the total NMHC reactivity in O_3 production was unchanged in the Tokyo metropolitan area between 1990 and 2010 despite its changeable composition. For estimating future O_3 levels, changes in the composition of VOCs in the ambient air and their reactivity should be considered. In addition, the sensitivity of O_3 production to precursors must be considered in future reduction measures. It was found to be VOC-sensitive in the target region, and the reduction in NMHC successfully proceeded with NO_x reduction, with a similar trend. However, their future changing rates might shift to NO_x sensitive or mixed sensitive and further influence the T-O_3 correlation pattern.

Authors' contributions
Hiroshi Yoshikado: overall study process from planning to fixing the manuscript, except introduction of reference papers by Dr. Kazuya Inoue and indication of insufficient arguing points by the anonymous reviewers.

Availability of data and materials
All data used in this study are publicly accessible via the websites of the National Institute for Environmental Studies, Japan, and the Japan Meteorological Agency.

Declarations

Competing interests
The author declares no competing interests.

References
Bloomer, B. J., Stehr, J. W., Piety, C. A., Salawitch, R. J., & Dickerson, R. R. (2009). Observed relationships of ozone air pollution with temperature and emissions. *Geophysical Research Letters, 36*, L09803. https://doi.org/10.1029/2009GL037308

Coates, J., Mar, K. A., Ojha, N., & Butler, T. M. (2016). The influence of temperature on ozone production under varying NOx conditions – A modelling study. *Atmospheric Chemistry and Physics, 16*, 11601–11615. https://doi.org/10.5194/acp-16-11601-2016

Garrido-Perez, J. M., Ordonez, C., Garcia-Herrera, R., & Schnell, J. L. (2019). The differing impact of air stagnation on summer ozone across Europe. *Atmospheric Environment, 219*, 117062. https://doi.org/10.1016/j.atmosenv.2019.117062

Inoue, K., Tonokura, K., & Yamada, H. (2019). Modeling study on the spatial variation of the sensitivity of photochemical ozone concentrations and population exposure to VOC emission reductions in Japan. *Air Quality, Atmosphere & Health, 12*, 1035–1047. https://doi.org/10.1007/s11869-019-00720-w

Inoue, K., Yasuda, R., Yoshikado, H., & Higashino, H. (2010). Spatial distribution of summer-time surface ozone sensitivity to NO_x and VOC emissions for the Kanto area part 1: Estimation by numerical simulations with two kinds of (lager and smaller) biogenic emission estimates. *Journal of Japan Society for Atmospheric Environment, 45*, 183–194. https://doi.org/10.11298/taiki.45.183. In Japanese with English summary.

Itahashi, S., Yumimoto, K., Uno, I., Ohara, T., Kurokawa, J., Shimizu, A., Yamamoto, S., Oishi, O., & Iwamoto, S. (2009). Analysis of transboundary air pollution occurred during spring 2007 over East Asia using CMAQ. *Journal of Japan Society for Atmospheric Environment, 44*, 175–185. https://doi.org/10.11298/taiki.44.175. In Japanese with English summary.

Kerr, G. H., Waugh, D. W., Strode, S. A., Steenrod, S. D., Oman, L. D., & Strahan, S. E. (2019). Disentangling the drivers of the summertime ozone-temperature relationship over the United States. *Journal of Geophysical Research: Atmospheres, 124*, 10503–10524. https://doi.org/10.1029/2019JD030572

Khiem, M., Ooka, R., Hayami, H., Yoshikado, H., Huang, H., & Kawamoto, Y. (2010). Process analysis of ozone formation under different weather conditions over the Kanto region of Japan using the MM5/CMAQ modelling system. *Atmospheric Environment, 44*, 4463–4473. https://doi.org/10.1016/j.atmosenv.2010.07.038

Kiriyama, Y., Hayami, H., Itahashi, S., Shimadera, H., Miura, K., Nakatsuka, S., & Morikawa, T. (2015). Effect of NO_x and VOC controls for surface ozone concentration in summertime in Kanto region of Japan. *Journal of Japan Society for Atmospheric Environment, 50*(8), 15. https://doi.org/10.11298/taiki.50.8

Kondo, H. (1990). A numerical experiment of the "extended sea breeze" over the Kanto plain. *Journal of the Meteorological Society of Japan, 20*, 687–694. https://doi.org/10.2151/jmsj1965.68.4_419

Kurita, H., & Ueda, H. (1986). Meteorological conditions for long-range transport under light gradient winds. *Atmospheric Environment, 20*, 687–694.

Ninneman, M., & Jaffe, D. (2021). Observed relationship between ozone and temperature for urban nonattainment areas in the United States. *Atmosphere, 12*, 1235. https://doi.org/10.3390/atmos12101235

Ooka, R., Khiem, M., Hayami, H., Yoshikado, H., Huang, H., & Kawamoto, Y. (2011). Influence of meteorological conditions on summer ozone levels in the Central Kanto area of Japan. *Procedia Environmental Sciences, 4*, 138–150. https://doi.org/10.1016/j.proenv.2011.03.017

Otero, N., Rust, H. W., & Butler, T. (2021). Temperature dependence of tropospheric ozone under NO_x reductions over Germany. *Atmospheric Environment, 253*, 118334. https://doi.org/10.1016/j.atmosenv.2021.118334

Porter, W. C., & Heald, C. L. (2019). The mechanisms and meteorological drivers of the summertime ozone–temperature relationship. *Atmospheric Chemistry and Physics, 19*, 13367–13381. https://doi.org/10.5194/acp-19-13367-2019

Pusede, S. E., Steiner, A. L., & Cohen, R. C. (2015). Temperature and recent trends in the chemistry of continental surface ozone. *Chemical Reviews, 115*, 3898–3918. https://doi.org/10.1021/cr5006815

Rasmussen, D. J., Fiore, A. M., Naik, V., Horowitz, L. W., McGinnis, S. J., & Schultz, M. G. (2012). Surface ozone-temperature relationships in the eastern US: A monthly climatology for evaluating chemistry-climate models. *Atmospheric Environment, 47*, 142–153. https://doi.org/10.1016/j.atmosenv.2011.11.021

Sakamoto, Y., Sadanaga, Y., Li, J., Matsuoka, K., Takemura, M., Fujii, T., Nakagawa, M., Kohno, N., Nakashima, Y., Sato, K., Nakayama, T., Kato, S., Takami, A., Yoshino, A., Murano, K., & Kajii, Y. (2019). Relative and absolute sensitivity analysis on ozone production in Tsukuba, a city in Japan. *Environmental Science and Technology, 53*, 13629–13635. https://doi.org/10.1021/acs.est.9b03542

Steiner, A. L., Davis, A. J., Sillman, S., Owen, R. C., Michalak, A. M., & Fiore, A. M. (2010). Observed suppression of ozone formation at extremely high temperatures due to chemical and biophysical feedbacks. *PNAS, 107*, 19685–19690. https://www.pnas.org/doi/10.1073/pnas.1008336107.

Ueno, H., & Tsunematsu, N. (2019). Sensitivity of ozone production to increasing temperature and reduction of precursors estimated from observation data. *Atmospheric Environment, 214*(715–721), 116818. https://doi.org/10.1016/j.atmosenv.2019.116818

Wakamatsu, S., Goi, K., Aburamoto, Y., Hatano, S., & Okuda, M. (1981). Relationship between the areal distribution of photochemical pollutants and

local wind flow covering Kanto district. *Journal of Japan Society of Air Pollution, 16*, 146–157.

Wakamatsu, S., Morikawa, T., & Ito, A. (2013). Air pollution trends in Japan between 1970 and 2012 and impact of urban air pollution countermeasures. *Asian Journal of Atmospheric Environment, 7*, 177–190. https://doi.org/10.5572/ajae.2013.7.4.177

Wakamatsu, S., Uno, I., Ohara, T., & Schere, K. L. (1999). A study of the relationship between photochemical ozone and its precursor emissions of nitrogen oxides and hydrocarbons in Tokyo and surrounding areas. *Atmospheric Environment, 33*, 3097–3108.

Yonemochi, S. (2019). Recent air pollution in summer in the Kanto area –O3 and PM25 in 2018-. *Earozoru Kenkyu, 34*, 65–72. https://doi.org/10.11203/jar.34.65. in Japanese with English summary.

Yoshikado, H. (1992). Numerical study of the daytime urban effect and its interaction with the sea breeze. *Journal of Applied Meteorology, 31*, 1146–1164. https://www.jstor.org/stable/26186555.

Yoshikado, H. (2013). Intense summer heat in Tokyo and its suburban areas related with variation in the synoptic-scale pressure field: A statistical analysis. *Journal of Applied Meteorology and Climatology, 52*, 2065–2074. https://www.jstor.org/stable/26175888.

Yoshikado, H. (2015). Summertime behavior of the precursors (non-methane hydrocarbons and nitrogen oxides) related with high concentrations of ozone in the Tokyo metropolitan area. *Journal of Japan Society for Atmospheric Environment, 50*, 44–51. https://doi.org/10.11298/taiki.50.44. In Japanese with English summary.

Yoshikado, H. (2021). How the high ozone concentrations in summer depend on air temperature. *Journal of Japan Society for Atmospheric Environment, 56*, 1–8. https://doi.org/10.11298/taiki.56.1. In Japanese with English summary.

Publisher's Note